Journal of Engineering Science and Technology Review 17 (4) (2024) 31- 39

Research Article

JOURNAL OF
Engineering Science and Technology Review

www.jestr.org

Radioclimatic Variable Characterization and Statistical Validation for Tropical Microwave Link Applications

Modupe E. Sanyaolu[1,*], Oluwafunmilayo O. Ometan[2], Felix O. Popoola[3], Sheu I. Owoyem[4], Ayodele O. Soge[1] and Alexander A. Willoughby[1]

[1]Department of Physical Sciences, Faculty of Natural Sciences, Redeemer's University, Ede, Osun State, Nigeria
[2]Department of Physics, Faculty of Sciences, Lagos State University, Ojo, Lagos State, Nigeria
[3]Department of Mathematical and Physical Sciences, Glorious Vision University, P.M.B. 001, Ogwa, Edo State, Nigeria
[4]Department of Integrated Science Adeyemi Federal University of Education, Ondo, Ondo State, Nigeria

Received 29 June 2023; Accepted 26 June 2024

Abstract

The main factor impairing radio wave propagation is atmospheric refraction. To account for fade margin, a crucial component of a reliable radio link, accurate estimates of the refractivity gradient and geoclimatic factor are vital for radio-wave signal transmission. In this study, three years of data from 2019 to 2021, collected from six distinct locations in Nigeria were utilized to analyse the radioclimatic variables to determine their influences on microwave linkages. The obtained values for surface refractivity show seasonal variation, with higher values during the wet season and lower values during harmattan. Makurdi, located in the north of the country, is mostly impacted by sub-refraction, whilst Lagos and Port-Harcourt, in the south, are impacted by super-refraction. The findings demonstrate that the shift of the intertropical discontinuity had an impact on how the seasons varied across the studied locations. The result would be an excellent tool for designing microwave wireless links in Nigeria.

Keywords: Fade margin, Geoclimatic factor, Microwave links, Propagation, Surface refractivity.

1. Introduction

The most accessible method for efficient propagation and communication uses radio links in the microwave frequency region [1]. They are utilized for the transmission of a sizable number of High-Definition Television (HDTV) channels with excellent audio and video output. Although operated at a greater operating frequency definition than television channels, this radio broadcast is nonetheless affected by a number of atmospheric factors [2]. It has been determined that the problem of climate change and rising global warming is caused by a net imbalance in the energy radiation of the earth [3].

To transmit high-quality messages, radio links must operate reliably and efficiently in light of the increased bandwidth demand that recent advancements in radio communication technology can support [4]. The troposphere has an impact on how radio waves travel between radio link terminals when using a wireless medium. When there are poor propagation conditions, the output signal will fluctuate, which will cause microwave links to fade [5]. Because of the extreme concentration of aerosol particles and other pollutants in industrial and heavily populated areas, the pollution in the atmosphere calls for attention [6]. The most frequent adverse impact on satellite communication lines at higher frequency bands is attenuation brought on by precipitation, especially in the tropical and equatorial regions [7].

More attention has been paid to the topic of radio refractivity, particularly in the temperate regions. A selection of these investigations includes those conducted by [8-10], to name a few. At Bern, Switzerland, and El Leoncito, Argentina, Andreas Lu¨di and Andreas Magun conducted research on the refractivity structure constant and length scales from mm-wave propagation in the stably stratified troposphere. They discovered that the Ozmidov scale L_R (proportional to Tatarskii's L_0) and the overturning turbulent length scale Lt could be determined simultaneously by measuring potential refractivity gradients (M) and outer scale lengths of turbulence in vertical and horizontal directions, respectively.

Based on the works of [11] and [12], and other researchers, the topic has recently begun to receive attention in the tropics. The tropical regions require significant attention because of their extreme climaticconditions. The impact of fluctuating tropospheric air temperature, relative humidity, and atmospheric moisture on UHF radio network propagation in the tropical region of south-western Nigeria was investigated by [13]. According to their analysis, the relationship between the received signal strength (RSS) and the variation in air temperature (control factor) can be used both technically and instrumentally to provide effective link control in the area. According to their findings, the three atmospheric characteristics have a major impact on UHF network links in the area.

Through the use of some polar-orbiting satellites and monthly data from [14] examined the variations of tropospheric refractivity, or N, over Nigeria. The data were retrieved from the archives of the department of Satellite Applications Facility for Climate Monitoring (CM—SAF) in Germany. The findings they made suggested that the Inter Tropical Discontinuity's (ITD) migration from north to south influences variations in every region and at various atmospheric heights. When the path loss has a positive slope,

*E-mail address: kemitidun@yahoo.com
ISSN: 1791-2377
doi:10.25103/jestr.174.05

it depends on the refractivity gradient; but, when it has a negative slope, it does not depend on it, according to Kim et al.'s analysis of the path loss features based on their Parabolic Equation model results [15].

In the modern era, where radio communications are heavily influenced by everything from mobile telephony to terrestrial digital broadcasting to the propagation of satellite radio signals through the troposphere, the behaviour of radio waves in the tropospheric layer of the Earth's atmosphere is extremely important. The troposphere causes radio waves to either bend upward which is known as sub-refraction or downward (diffraction) to the Earth's surface, which results in abnormal propagation called super refraction and ducting [16]. The performance of radio communication lines and radar is significantly impacted by these factors [17-18].

Refractivity is one of the main challenges of radio propagation due to non-uniform medium of the atmosphere [19]. To maximize the effectiveness of a microwave link, some parameters including the effective earth radius factor (k), and the point refractivity gradient must be carefully tuned. Atmospheric weather parameters such as temperature, relative humidity, and dew point vary in time and space, these in turn cause variations in the geoclimatic factor. A measurement of a terrain's climatic and geographic conditions is called the Geo-climatic Factor (K) [20]. Geoclimatic factor play a vital role in the procedure for calculating the percentage of time when a particular fade depth is exceeded. The effective earth radius (k factor) along with the changes to the geoclimatic factor causes radio signals to refract in diverse routes over the curvature of the earth causing multipath fading of the radio signal [21]. The frequency, hop length, type and roughness of the terrain, weather, and path clearance are factors that affect multipath fading outages [22]. The importance of determining the geoclimatic factor based on each site and region of interest can therefore not be overstated. Appropriate planning is also required in order to guarantee that terrestrial radio links transport radio waves successfully.

Various methods have been suggested by numerous authors to address this issue with radio propagation in various parts of the world. The radio propagation data of the relevant locations were used to create these strategies [23–26]. The geoclimatic factor, which is the primary effect for both the suggestive of geographical and climatic aspects of the region of interest, is crucial, according to those researchers [23].

Scientists have proposed several practical empirical models that are based on a large amount of atmospheric refractivity measurement data. These models include an exponential model, a linear model, and a piecewise model

Exponential model

After conducting a statistical study on extensive long-term measurement data collected across several regions, researchers have discovered that an exponential model can accurately represent the average air refractivity. By computing the annual or monthly average, as shown by Equation 1, which yields a standard deviation smaller than 5 N units, a low error rate is guaranteed.

$$N(h) = N_s + \Delta N \, x \, (h - h_s) \quad (1)$$

$$N(h) = N_1 exp[-C_e(h - h_s - 1)] \quad (2)$$

Where C_e can be obtained from equation 3

$$C_e = ln\left(\frac{N_s}{N_s+\Delta N}\right) \quad (3)$$

Linear model

The linear model is expressed as:

$$N(h) = N_s + \Delta N \, x \, (h - h_s) \quad (4)$$

Where N(h), N_s, ΔN, h and h_s represent the atmospheric refractivity at a certain height h, refractivity at ground level, gradient of the atmospheric refractivity, altitude above sea level in meters and the location height above sea level also in meters. According to [27] reported that statistical results based on substantial measurement data indicate that the actual relation between ΔN and Ns is as specified in in equation 5.

$$\Delta N = -7.32 \exp(0.005577 N_s) \quad (5)$$

According to the data, this linear model shows good agreement with reality for heights less than one kilometer above sea level. If the altitude is higher than this range, the model becomes less accurate.

Piecewise model

Additionally, scientists have put forth a piecewise model. Equation 6 illustrates how this more accurately characterizes the variations in air refractivity with height.

$$N(h) = \begin{Bmatrix} N_s + \Delta N \, x \, (h - h_s) h_s \le h \le h_s + 1 \\ N_1 exp[-C_1(h - h_s - 1)] h_s + 1 < h < 9 \\ 105 exp[-0.1424(h-9)] 9 \le h \le 60 \end{Bmatrix} \quad (6)$$

where C_1 is the exponential attenuation coefficient between 1 and 9 km and may be derived using equation 5. where N_1 is the atmospheric refractivity at 1 km above sea level, and ΔN is the gradient of the atmospheric refractivity up to 1 km above sea level.

$$C_1 = \frac{1}{8-h_s} ln \frac{N_1}{105} \quad (7)$$

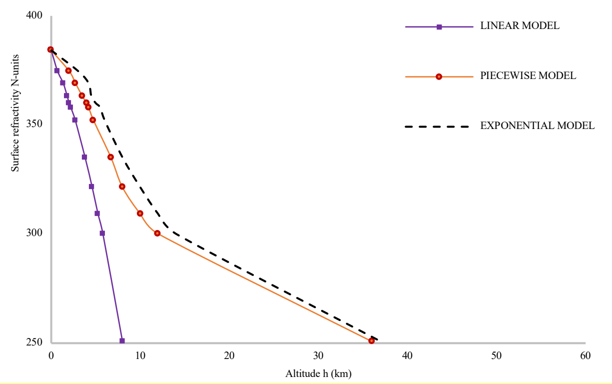

Fig. 1. Comparison of the curves for Linear, Piecewise and Exponential models

Figure 1 presents a comparison of the curves for these three models assuming a surface refractivity of 345 N-units. An ITU (International Telecommunications Union) recommendation, which is primarily used for this study, is the basis for the surface refractivity value. It is evident that the piecewise model and the exponential model are extremely similar. As one ascends above sea level, h, the linear model rapidly separates from the others. The linear model's atmospheric refractivity turns negative for h values greater than 8 km, while the outcome loses significance for h values less than 3 km. [28]

The radio refractivity index N is defined by the International Telecommunication Union (ITU). The model adopted for this study is ITU-R, 453-12 [29] it expressed refractivity N (p, e, T), where p is the total atmospheric pressure, e is the vapour pressure, and T is the ambient temperature [29] as:

$$N = 77.6\frac{p}{T} + 3.75\ X\ 10^5\frac{e}{T^2} - 5.6\frac{e}{T} \quad (8)$$

Equation 7 consist of two equations where

$$N = N_{dry} + N_{wet}$$

$$N_{dry} = 77.6\frac{p}{T}$$

$$N_{wet} = 3.723\ X\ 10^5\frac{e}{T^2}$$

T is measured in Kelvin, p and e are measured in hPa. As can be seen from Equation (7), the amount of moisture in the atmosphere has a significant impact on atmospheric radio refractivity. The term N_{dry} is used for calculating the dry season periods (usually November to January) and N_{wet} for wet seasons (February to October). It should also be emphasized that Equation (1) is accurate and dependable for calculating the refractivity of a wide range of frequencies, valid for radio frequencies up to 100 GHz [30-31], making it a typical model for calculating radio refractivity.

The effective earth radius factor, also known as the k-factor, is a number that is used to categorize radio refractivity into categories including normal or standard refraction, sub-refraction, super-refraction, and ducting. Calculating the k factor is expressed by [32].

$$k = \left(1 + \frac{\frac{dN}{dh}}{157}\right)^{-1} \quad (9)$$

where $\frac{dN}{dh}$ is the refractivity gradient

$$\frac{dN}{dh} = \frac{N_s - N_h}{h_2 - h_1} \quad (10)$$

According to climate, season, transitory weather conditions during the day, congestion, and terrain throughout the communication line, refractivity gradients can vary [33]. The radio signal bends toward the ground and travels beyond the geometric horizon when refractivity gradients is negative (beyond 100 N-unit/km).

The aim of this study is to characterized the radio climatic variables which include, the surface refractivity, radio refractivity gradient, effective earth radius, and geoclimatic factor in six selected locations in Nigeria. Since Nigeria is a tropical country with severe weather effects during the rainy and dry seasons. The unpredictable environment that radiowave signal is traveling through necessitates this investigation.

2. Nigeria Climate

Nigeria is situated between latitudes 4° and 14° N and 2° and 15° E, respectively. The country is close to both the equator and the cancer tropics. In general, Nigeria has an equatorial and tropical continental climate. Nigeria's climate is truly tropical, with average temperatures ranging from 24°C to 27°C and an annual mean temperature of 27°C in the tropical rainforest to the south but a higher mean value in the sub-Sahel to the north. This is due to the movement of the Inter Tropical Discontinuity (ITD) in combination with aspects of ocean atmosphere coupling. Table 1 shows the climatic zone characteristics of the study locations. A long dry season, lasting from October to mid-May, is followed by a brief rainy season, lasting from June to September, with an annual mean of roughly 50 cm. However, the southern region has a lengthy wet season (March through October), with the heaviest rain falling in June or July.

Yola is located in Nigeria's northeast and exhibits some Sahel savannah characteristics. The area has two different seasons: the dry season and the rainy season. The wet season typically begins in early June and lasts through early October, with the dry season starting around November and ending around May. Despite the brief duration of the rainy season, it always rains very heavily throughout this time. Due to the north-easterly wind coming from the Sahara Desert, the area also gets Harmattan dust between December and February.

Tropical weather prevails in Lagos, which is located in the South-west of Nigeria. Port Harcourt in the South-South has an uncommon type of climate known as the tropical monsoon, is comparable to Lagos. Almost the entire year is marked by precipitation in these two places. All through the year, the temperature is rather consistent. The harmattan is noticeably less evident in the two metropolis, despite the fact that it still greatly affects the weather across West Africa.

Makurdi, located within the guinea savannah region was selected due to its nature. Makurdi is scorching hot. This region experiences a wet season that lasts from April to early October. From November until April is the dry season. From late December to early February, this area is also filled with the harmattan dust.

Ayingba has a tropical hinterland climate, which is characterized by a small diurnal temperature range, high humidity, and a growing cumulus cloud cover from March to early April. Rainfall occurs as brief, sharp showers and thunderstorm activity, which are signs of the beginning of the rainy season.

The savannah climate of Oshogbo is tropical. The city experiences two main seasons (dry and wet), which are typical of the monsoon climate in West Africa and are indicated by a clear seasonal shift in the wind pattern. It is influenced by the moist maritime south-west monsoon breeze that comes inland from the Atlantic Ocean between March and October. The Sahara Desert's dry, dusty winds blow throughout the dry season, which lasts from November to February. The strongest harmattan winds, which are dry and dusty, occur between December and January.

3. Methods

As shown in Table 1, the places considered for this study include the various climate zones in Nigeria. The three years (2019 to 2021) data collected for this work were from the measurement of the meteorological parameters: atmospheric pressure, temperature, water vapour, and relative humidity which were obtained from six stations in Nigeria, shown in Figure 1; Makurdi, Lagos, Port-Harcourt, Yola, Ayingba, and Oshogbo, which were all up to 100 m above sea level using the Era 5 Satellite. The data were validated using the meteorological data from the Tropospheric Observatory Data Network (TRODAN) of Nigeria.

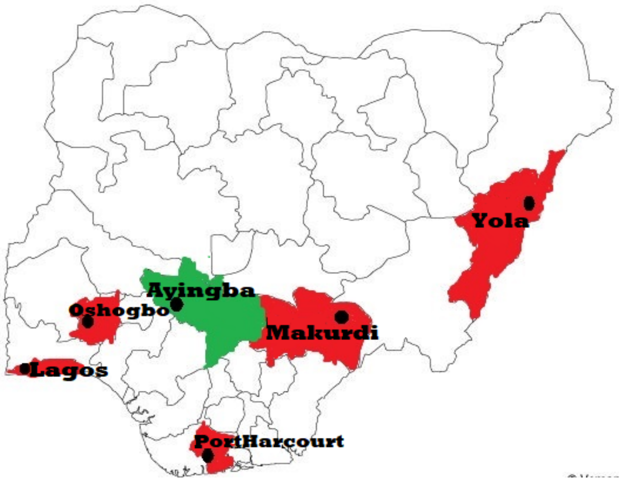

Fig. 2. Map of Nigeria showing selected locations

Equation 7 was used to calculate the surface refractivity. The surface refractivity, which corresponds to altitude h_s, and level refractivity, N_h (100 m), which corresponds to altitude h, were combined to estimate the refractivity gradient $\frac{dN}{dh}$. As a result, the radio refractivity gradient which is often given in units/km, is expressed by [34]:

$$\frac{dN}{dh} = \frac{N_s - N_h}{h_2 - h_1} \quad (11)$$

N_s and N_h are radio refractivity values at heights h_2 and h_1, respectively.

The Geoclimatic factor was calculated using [34] given as:

$$K = 10^{-4.2-0.0029(\frac{dN_1}{dh})} \quad (12)$$

Table 1. Geographic and climatic characteristic of study areas

Stations	Longitude	Latitude	Annual Mean Precipitation (mm)	Average Temperature (ºC)	Climatic Region
Makurdi	8.92º E	7.75"N	1,290	28.26182	Guinea Savanna
Lagos	3°26'1.19"E	6°48'3.77"N	1,540	26.62534	Tropical
Port-Harcourt	6°54'2.58"E	4°43'6.18"N	2,719	26.98320	Tropical Monsoon
Yola	12°28'4.47"E	9°12'3.30"N	114.29	30.53711	Tropical Savanna
Ayingba	7°10'2.10"E	7°29'3.12"N	654.21	26.79148	Tropical Hinterland
Osogbo	4°32'3.59"E	7°46'5.61"N	1,361	26.58866	Tropical Savanna

4. Result and Discussion

The results of the collected data from the years 2019 to 2021 are presented in Tables 2 and 3 shows the estimation of monthly average values of geoclimatic factor and effective factor of the earth radius (k) over the study period across the six selected stations. The graphs of annual fluctuations of surface refractivity on a monthly basis for the cities of Makurdi, Oshogbo, Yola, Lagos, Ayingba, and Port -Harcourt are shown in Figures 2-6.

Table 2. Estimated monthly average values of geoclimatic factor and effective earth radius k over the study period across Yola, Makurdi and Oshogbo based on meteorological data.

	Yola		Makurdi		Oshogbo	
Months	***Geoclimatic Factor, K*** $(\times 10^{-5})$	***Effective radius, k factor***	***Geoclimatic Factor, K*** $(\times 10^{-5})$	***Effective radius, k factor***	***Geoclimatic Factor, K*** $(\times 10^{-5})$	***Effective radius, k factor***
Jan	3.56	2.1957	3.86	1.8816	4.31	1.5702
Feb	4.89	1.3202	3.09	3.1339	2.19	5.3641
Mar	3.58	2.1768	4.70	1.3899	3.21	2.8124
May	4.74	1.3758	4.57	1.4405	4.37	1.5407
Jun	4.57	1.4426	4.52	1.4651	3.23	2.7745
Jul	4.53	1.4609	3.67	2.0639	3.99	1.7797
Aug	4.67	1.4009	4.50	1.4734	4.43	1.5092
Sept	4.54	1.4558	4.50	1.4740	4.43	1.5079
Oct	3.7	2.0334	3.66	2.0734	2.65	5.8405
Nov	3.34	2.5369	4.24	1.6105	4.13	1.6802
Dec	4.69	1.3951	4.46	1.4913	4.39	1.5298

Table 3. Estimation of monthly average values of geoclimatic factor and effective earth radius k over the study period across Port-Harcourt, Lagos and Ayingba.

	Port-Harcourt		Lagos		Ayingba	
Months	***Geoclimatic Factor, K*** $(\times 10^{-5})$	***Effective radius, k factor***	***Geoclimatic Factor, K*** $(\times 10^{-5})$	***Effective radius, k factor***	***Geoclimatic Factor, K*** $(\times 10^{-5})$	***Effective radius, k factor***
Jan	3.72	2.0080	2.89	3.9169	3.93	1.8230
Feb	3.03	3.3067	2.65	5.7569	4.63	1.4195
Mar	2.46	9.5649	3.29	2.6307	2.76	4.7312
May	3.73	1.9971	4.49	1.4792	4.58	1.4400
Jun	3.37	2.4859	4.48	1.4847	4.67	1.4026
Jul	3.68	2.0479	4.48	1.4832	4.54	1.4569
Aug	3.73	2.0011	2.69	5.3345	4.56	1.4484
Sept	2.47	9.3591	3.67	2.0676	2.46	9.6962
Oct	3.03	3.3087	4.49	1.4785	4.5	1.4752
Nov	3.73	1.9972	4.32	1.5629	3.71	2.0236
Dec	3.39	2.4533	4.48	1.4814	3.63	2.1141

Figure 3(A) shows the estimated monthly surface refractivity values as they vary for the years 2019-2021 in Lagos. The range of refractivity values are between 378 and 317 N-units. Lagos refractivity values for the harmattan months (November, December, January, and February,) are between 305 and 338 N-units, but for the wet season months (March to October), the values are between 378 and 321 N-units.

Figure 3(B) demonstrates that throughout the examined years in Makurdi, surface refractivity normally grew progressively from January to May. The month of October sees a steady rise after that, followed by a sharp decline in the month of December. The lowest refractivity value of 290 N-units was recorded for December 2020, while the month of July (2021) a typical month during Nigeria's rainy season—recorded the highest value of 379 N-units. It is also observed that surface refractivity is often higher from April to October, when it rains more frequently. This might be caused by the high air relative humidity that was recorded in Makurdi at the time. Due to South to North motion of the inter-tropical discontinuity (ITD) with the Sun, Makurdi may be affected by the moist tropical marine air during this time. Surface refractivity decreased in December because the dry harmattan and dominant northeasterly winds during this time became more prevalent, which is why low surface values were seen in January and February. However, between April and October, widespread rainfall was predominant, causing a rise in atmospheric moisture, due to increase in humidity, and as a result, surface refractivity is increased reaching its peak of 383

N-units in May

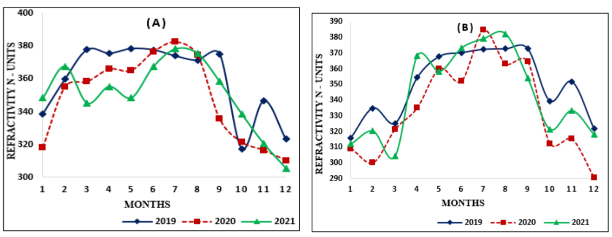

Fig. 3. Surface refractivity in (a) Lagos and (b) Makurdi

Port-Harcourt is shown in Figure 4(A) as having monthly refractivity fluctuation for the years 2019 to 2021. The refractivity values are between 328 and 348 N-units in the stations' harmattan months (January, February, November, December) which are the low refractive values of the observation period. However other seasonal fluctuations of refractivity are also seen., as the average monthly refractivity values recorded for the raining season are 377 and 388 N-units.

Figure 4(B) depicts the change in Yola's monthly surface refractivity during the course of the study. Following the analysis and presentation of the fluctuations in surface refractivity over Yola for a three-year period, the refractivity values during the non-rainy months of January, February, November, and December are low, ranging from 292 N-units to roughly 295 N-units. The statistics for these months show the substantial influence of the dry continental air mass that dominates throughout the dry season as a result of ITD's North-South migration; as a result, these months show pronounced variance. Low moisture content results from a combination of low humidity and high temperature values, which lowers refractive values. Refractive index values between 375 and 358 N units are seen during the wet (rainy) season, which runs from March to October, compared to those for the harmattan months. It has been noted that the refractivity values are higher than those recorded for the harmattan season.

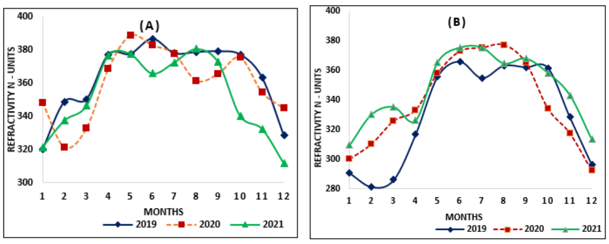

Fig. 4. Surface refractivity in (A) Port-Harcourt and (B) Yola

Figure 5(A) depicts the average monthly fluctuation in refractive index for the years 2019 to 2021 in Ayingba, which is 385 metres above sea level. Again, a similar pattern of seasonal fluctuations is observed, with the harmattan months of January, February, November, and December having the lowest refractive indices having a 298–315 N-unit range in the refractivity values. In March 2020, a considerable increase was seen, with a refractivity value of 300 to 356 N-units. The refractivity values is increasing for the wet season months of April, May, June, July, August, September, and October range from 363 to 380 N-units.

The mean monthly Ns variations in Oshogbo, which is located 320 metres above mean sea level, are shown in Figure 5(B) for the years 2019 to 2020. The dry (non-rainy) season months of January, February, November, and December had the lowest refractivity ratings. Between 320 and 342 N-units is the range for the refractivity values. May, June, July, August, September, and October are the months that fall within the wet season and have refractivity values that range from 378 to 381 N-units. According to the findings, the stations are experiencing similar meteorological circumstances caused by the ITD's N-S migration [25].

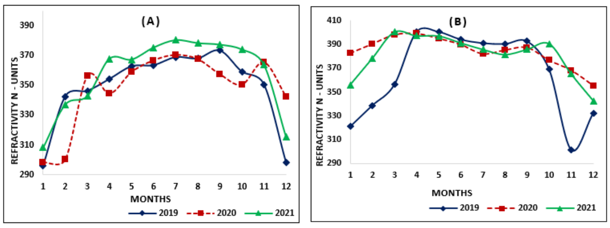

Fig. 5. Surface refractivity in (A) Ayingba and (B) Oshogbo

The spatial distribution of the average radio refractivity gradient and the k factor are shown in Figures 6 and 7. Figure 5 shows that the atmosphere of Nigeria is dominated by two main types of refraction: sub-refraction, which occurs when the radioactivity gradient is greater than 40 N-units/km or infinity less than the k factor and less than 1.33, and super-refraction, which occurs when the radioactivity gradient is less than 40 N-units/km or zero greater than the k factor and more than 1.33. While Lagos and Port Harcourt in the south of Nigeria are afflicted by super-refraction, Makurdi in the north of the country is primarily affected by sub-refraction.

As observed in Figure 6, Makurdi and Yola have an average refractivity gradient value of -35.2 and -30.62 N-units/km with a k factor of 1.30 and 1.32 respectively. The refractivity gradient average values for Lagos, Port Harcourt, Oshogbo, and Ayingba are -81, -93, -68 and -70 N units respectively with k factor of 1.42, 1.51, 1.73 and 1.50 respectively.

Moreover, Figure 7(B) shows that, in accordance with seasonal variations in moisture, the k-factor increases and the refractivity gradient decreases throughout the wet season. It is also observed from the Figure that sub-refraction typically occurs at higher latitudes in Nigeria as seen for Yola and Makurdi in Table 1 while super-refraction typically occurs at lower latitudes.

The link must include a fade buffer that accounts for multipath fading when designing the terrestrial line of sight systems. The frequency of operation, path length, path inclination, and the geo-climatic element of the studied location are all taken into account by the International Telecommunication Union recommendations (ITU-R) [34] suggested multipath fading. The geo-climatic component has a direct relationship with the fade margin. The K value derived from local data, according to ITU-R, yields a precise estimate of multipath fading.

Knowing the geoclimatic factor value in a month in which poor reception of radio signal is experienced is a crucial factor in determining the multipath fade margin. This relates to the month where K has the highest value. Figure 6 depicts the geo-climatic factor's monthly variance for each of the six cities included in the study. K reaches its highest value for Makurdi in the months of March and April, with a peak of K = 0.000047 in March. In Lagos, the months of April and October have the highest K values, totalling K = 0.000044. Between July and October, Port Harcourt experiences its highest K values, with a peak of K = 0.000038. Between February and November, Yola experiences its highest K values, with a peak of K = 0.000048 in February. Additionally, K levels in Ayingba are high in February and May, with the greatest value of K being 0.000047 in May. The high K values for Oshogbo were between April and August. having the highest value of 0.000044 occurring in April. As a result, considering all the location under this study, the geoclimatic values of Yola is higher than any other location and consequently its multipath fading will be more.

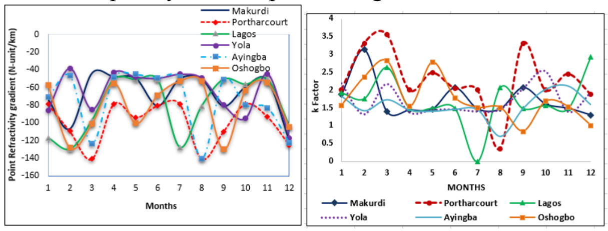

(a) (b)

Fig. 6. (a) Refractivity gradients and (b) Effective earth radius factor across study locations

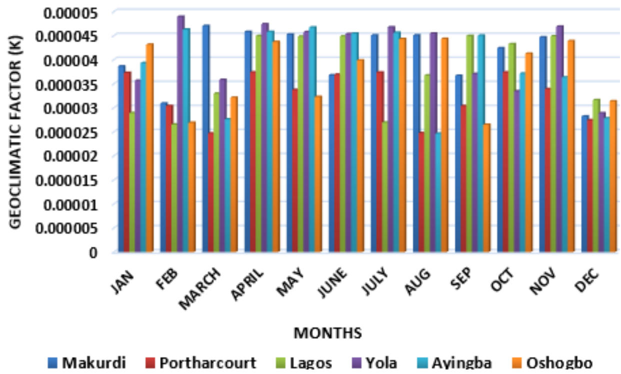

Fig. 7. Mean monthly values of geoclimatic factor across the studied locations

Figure 8(A) shows the comparison of the surface refractivity using Era5 satellite data and the TRODAN ground data in Makurdi. The plot shows that with both TRODAN and Era5 predicted low in the dry season while the value of surface refractivity was high during the raining season (from March to September). In January 2019, data from Era 5 predicted 315 N units while 309 N-units were predicted for TRODAN. Era5 data predicted 309 N-units while TRODAN gave 300 N-units in January 2020. 312 N-units were obtained from Era5 satellite data in 2021 while 300 N-units were predicted from TRODAN data. Generally, in Makurdi, Era5 data predicted a little higher than the ground data except for September where Refractivity value from the ground data attained the highest value of 390 N units and Era5 data gave 369 N- units.

In Figure 8(B), similar trend was observed in Port-Harcourt. In 2020, the refractivity values were as high as 340 N-units from Era5 data while 321 N-units were obtained from the ground data. Surface refractivity were seen to be low from observation in the dry season of 2019 to 2021 both from Era5 and TRODAN data and thereafter increased gradually, reaching its peak in August.

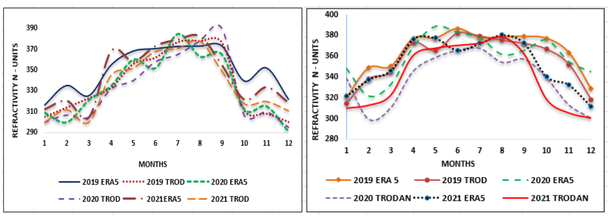

(a) (b)

Fig. 8. Validation of the surface refractivity using Era5 satellite data and the in-situ TRODAN ground data in (A) Makurdi and (B) Port-Harcourt

Seasonal Statistical Trends

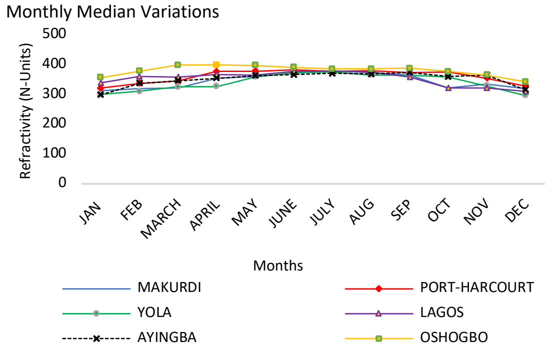

Fig. 9. Monthly median variations of surface refractivity in selected locations

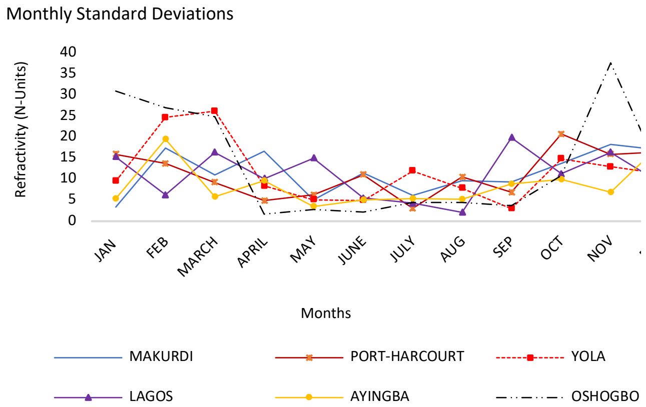

Fig. 10. Monthly standard deviation of surface refractivity in selected locations

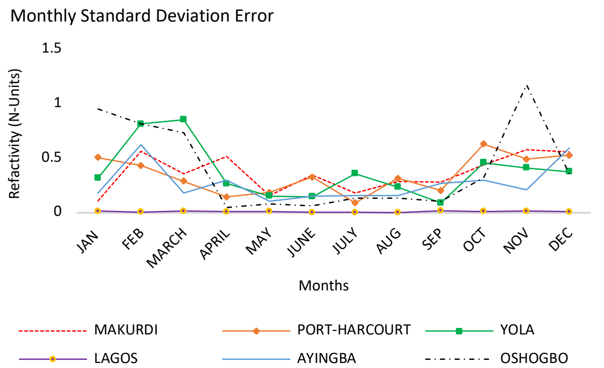

Fig. 11. Monthly standard deviation error of surface refractivity in selected locations

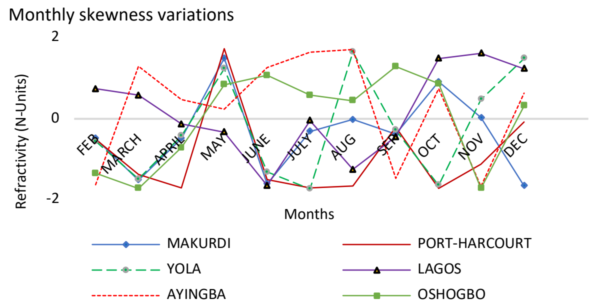

Fig. 12. Monthly skewness variations of surface refractivity in selected locations

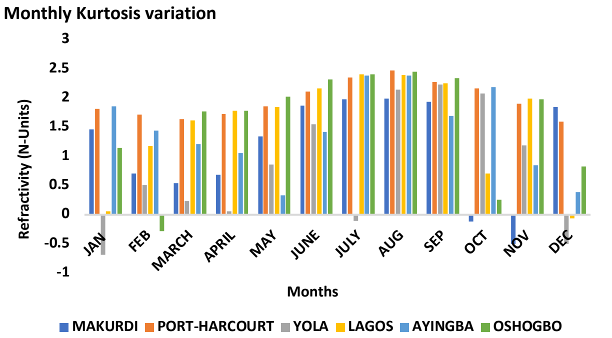

Fig. 13. Monthly kurtosis variations of surface refractivity in selected locations

Figure 9 to Figure 13 shows the statistical trends of surface refractivity across the six selected locations. The median, standard deviation, standard deviation error, skewness and kurtosis were analysed.

The monthly average surface refractivity value fluctuates from 340.120 N-unit / km in February, which is found over Port-Harcourt and Lagos, to 356.341 N-unit / km in May, which is distributed over Ayingba, Oshogbo, and Yola throughout the wet season (February to October). During this season, Lagos' monthly standard deviation value was determined to be close to 37.66 N-unit/Km). Super-refractive conditions are found in the range of 376.66 N-unit/Km in March, 315.50 N-unit/Km in April, and 329.330 N-unit/Km in May throughout this wet season, according to the median variations. With the exception of Oshogho, which has a peak value of 1.17, all locations have extremely low standard deviation errors. The super-refractive circumstances in March were -1.006 N-unit/Km, April was -1.22 N-unit/Km), and May recorded -1.104 N-unit/Km as revealed by the kurtosis. The monthly refractivity's skewness revealed that these distributions are right-skewed, with the majority of super-refractive condition values concentrated to the left of average values.

In March, the median value was 334.386 N-units/Km, which was found over Yola, Makurdi, and Oshogbo, and Ayingba; in April, it was 383.07 N-units/Km, which was found over Lagos and Port-Harcourt; and in May, it was 378.11 N-units/Km, which was located around Oshogbo. During this season, we have seen a strong monthly link between super-refractive circumstances. During these months of this season, the correlation values were 0.76 N-unit/Km, 0.89 N- unit/Km, and 0.68 N-unit/Km).

The monthly median readings for June (Lagos) were 318.88 (M/Km), July (Port-Harcourt) was 282.72 (N-unit/Km), August (Makurdi) was 314.15 (N-unit/Km), and September (Yola) was 239.67 (N-unit/Km). The monthly refractive distributions were flat skewed during this season, as demonstrated by the monthly kurtosis value, which is 1.0 N-unit/Km. The left side of the average values contained the majority of the refractivity values that produced the super-refractive situations. There was a very strong connection in the refractive conditions this season, of about 0.83 (M/Km).

The start of the dry season and its climax occur from November to January. Examining the statistics for this season was quite fascinating, particularly when looking at the median fluctuation. The average value for median variation of, after 313.167 N-unit/Km in November, was found in December (278.07 N-unit/Km and spreading over Port-Harcourt, Lagos, Ayingba and Oshogbo.), while the lowest average value for refractive conditions was found in January 255.06 N-unit/Km and over Yola and Makurdi. This is in agreement with the works of [14] and [15].

A narrow distribution of these refractive conditions around their monthly average super-refractive conditions is indicated by the standard deviation of values 4.86 N-unit/Km in November in Ayingba and Oshogbo followed by values of 7.34 and 9.344 N-unit/Km in December in Port-Harcourt and Lagos respectively. According to the monthly kurtosis values for the refractive conditions, which were 1.73 N-units/Km in November and 1.439 N-units/Km in October, the refractive conditions during this season follow the same distributions for the median, and skewness.

5. Conclusion

In this work, the surface refractivity, refractivity gradient, geoclimatic factor K, and associated k-factor which are crucial radio climatic variables in the planning of the radio links for six stations in Nigeria have all been estimated. The study shows that values of surface refractivity changes with season, higher values were characterized with the raining season while the harmattan season is characterized with lower values. It is also observed that as the values of refractivity gradient become more negative, the Geo-climatic factor increases.

The statistical trend shows that the monthly kurtosis values for wet season adhere to the same distributions as those for the dry season. This indicates that there were not particularly significant super-refractive conditions throughout the dry season. A narrow distribution of these refractive conditions around their monthly average super-refractive conditions is indicated by the standard deviation of values. We can infer from the monthly skewness number that right-skewed distributions happened during the beginning of the dry season and moved towards the left at the beginning of wet season and then became almost same for every other month.

The TRODAN ground data was also used to validate the Era5 satellite data. The outcome demonstrates that there is good agreement between the two data sources in forecasting radio climatic variables in the studied areas.

The overall finding will be helpful in determining the location-dependent fade margins needed for radio propagation purposes, both for terrestrial and satellite communication in the studied areas in Nigeria.

Acknowledgements

The support of the Centre for Atmospheric Research (CAR), and National Space Research and Development Agency (NASRDA) are appreciated for their support in providing the TRODAN weather stations to access the data used for this study.

References

[1] I. Emmanuel, B. Adeyemi, and D. Adedayo, "Estimation of Refractivity Gradient and Geoclimatic Factor for Radio Link Design in Nigeria," *Phys. Sci. Int. J.,* vol. 19, no. 2, pp. 1-9, Aug. 2018, doi:10.9734/PSIJ/2018/34489

[2] A. O. Aremu, and J. A. Mufutau, "Influence of Geoclimatic Factor on Fade Depth for Wireless Link Design using Radiosonde Data," *Int. J. Res. Sci. Innov. Appl. Sci.,* vol. 5, no 9, pp 143 -146, Sep. 2020

[3] M. Sanyaolu, "Distribution of seasonal variation of point refractivity gradient and geo-climatic factor over Ede-Nigeria", *Songklanakarin J. Sci. Technol*, vol. 45, no 2, pp. 250–255, Sep. 2023.

[4] A. T. Adediji, M. O. Ajewole, S. E. Falodun, and O. R. Oladosu, "Radio refractivity measurement at 150 m altitude on TV tower in Akure, South West Nigeria", *J. Eng. Appl. Sci*., vol. 2, no. 8, pp. 1308 – 1313, Jan. 2007.

[5] D. R. Siddle, E. M. Warrington., and S. D. Gunashekar, "Signal strength variations at 2 GHz for three sea paths in the British Channel Islands: Observations and statistical analysis", *Radio Sci*., vol. 42, no. 4, pp. 1-13, Aug. 2007.

[6] R. Waleed. Al-Rijaboa , A. Basheer, and M. Banoosh, "Spatial and Temporal Variation of Clearness Index in Iraq", *Jordan J. Phys*, vol. 14, no. 2, pp. 129-138, Jun. 2021, doi 10.47011/14.2.4

[7] E. Modupe Sanyaolu Modupe, "Performance of Rain- Induced Attenuation Prediction Models for Terrestrial Link in Cameroon," *Int. J. Eng. Appl. Sci. Tech.,* vol. 7, no 1, pp 17-25, May 2002.

[8] N. R. Dhein, M. S. Pontes, and M. L. Silva, "Statistical behavior of refractivity gradient in the tropics," *IEE Conf. Publication,* London, No. 370, pp 340-343, Sep. 1993.

[9] Řezáčová Daniela, Ondřej Fišer and Lucas Ramón Sáez, "Statistics of Radio Refractivity Derived from Prague Radio sounding Data," *Radio Eng.*, vol 12, no 4, pp 84-86, Dec. 2003.

[10] Z. Valma, M. Tamosiunaite, S. Tamosiunas, M. Tamosiuniene and M. Zilinskas, "Variation of radio refractivity with height above ground," *Int. J. Electr. Electron. Telecommun. Eng.,* vol. 111, no. 5, pp. 23-26, Jun. 2011, doi: 10.5755/j01.eee.111.5.349

[11] B. Adeyemi and I. Emmanuel, "Monitoring tropospheric radio refractivity over Nigeria using CN-SAF data derived from NOAA-15, 16 and 18 satellite," *Indian J. Radio Space Phys.*, vol. 40, pp. 301- 310, Dec. 2011.

[12] K. C. Igwe, and I.A. Adimula, "Variation of surface radio refractivity and radio refractive index gradients in the sub-Sahel," *Nigeria J. Space Res.*, vol. 6, pp 135-144, May 2009.

[13] E. P. Agbo, E. B. Ettah, and E. E. Eno. "The impacts of meteorological parameters on the seasonal, monthly and annual variation of radio refractivity," *Indian J. Phys*., vol. 95, no. 2, pp. 195–207, Feb. 2021, doi: 10.1007/s12648-020-01711-9

[14] M. E. Sanyaolu, O. F. Dairo, A. A. Willoughby, and L. B. Kolawole, "Estimation of Rain Fade Durations on Communication Links at Ka-band in Equatorial and Tropical Regions," *Telecommun. Radio Eng.*, vol. 79, no. 2, pp 129-141, Jul. 2020, doi: 10.1615/TelecomRadEng.v79.i2.50

[15] J. Kim, Y. Kim, J. Lee, and Y. Choi, "Analysis of pathloss characteristics with variation of refractivity gradient using the parabolic equation" *Jong Ho Kim's Lab,* pp 1-11, Jul. 2014.

[16] I. Sirkova and M. Mikhalev, "Parabolic-equation based study of ducting effects on microwave propagation", *Microw. Opt.Technol. lett.*, vol. 42, no. 5, pp 390 – 394, Jul. 2004, doi: 10.1002/mop.20314

[17] M. P. M. Hall and Institution of Electrical Engineers, Eds., *Propagation of radiowaves*. London: Institution of Electrical Engineers, 1996.

[18] E. Sanyaolu Modupe, "Laser Communication and Atmospheric Impairments", *Global Sci. J.*, vol. 9, no. 10, pp. 181-191. Oct. 2021.

[19] M. E. Sanyaolu, and O. Sanyaolu, "Seasonal and latitudinal variations of surface radio refractivity over Nigeria", *Indones. J. Electr. Eng. Comput. Sci.*, vol. 28, no. 3, pp. 1548-1553, Dec. 2022, doi: 10.11591/ijeecs.v28.i3.pp1548-1553

[20] T. Tjelta, R. L. Olsen, and L. Martin, "Systematic development of new multivariable techniques for predicting the distribution of multipath fading on terrestrial microwave links", *IEEE Trans. Anten. Propag*, vol 38, pp. 1650-1665, Oct. 1990, doi: 10.1109/8.59780

[21] O. L. Ojo, O. Ajewole, A.T. Adediji, and J. S. Ojo, "Estimation of clear-air fades depth due to radio climatological parameters for microwave link applications in Akure, Nigeria", *J. Eng. Appl. Sci.*, vol, 7 no 3, Aug. 2015.

[22] Y. Bettouche, B. Agba, A, B. Kouki, H. Obeidat, A. Alabdullah, F. Abdussalam, S. Ghauri, S., and R. A. Abd-Alhameed, "Estimation and Analysis of the Radio Refractivity, its gradient, and the

Geoclimatic factor in Arctic Regions", *Prog. Electromagn. Res*. C., vol. 92, pp. 181-192. May 2020. doi: 10.2528/PIERM20020709

[23] O. D. Oyedum, "Duct-Induced terrestrial microwave link degradation in Nigeria: Minimization factors", *Indian J. Radio Space Phys*., vol 41, no 3, pp 339-347, Jan. 2012.

[24] Davidson, Akpootu, and M. Iliyasu, "Estimation of Tropospheric Radio Refractivity and Its Variation with Meteorological Parameters over Ikeja, Nigeria," *J. Geogr. Environ. Earth Sci. Int.*, vol. 10, 1, pp 1-12, May 2017, doi: 10.9734/JGEESI/2017/32534

[25] B. Adeyemi, and I. Emmanuel, "Radio refractivity gradient over Nigeria using CM – SAF satellite retrieved data," *Nigerian J. Technol. Res.*, vol. 7, no 2, Dec. 2012, doi: 10.4314/njtr.v7i2.83782

[26] J. S. Ojo, L. Olalekan, and O.V. Omole, "Application of Spatial interpolation technique for the determination of Geoclimatic factor and fade depth using Secondary variables for microwave applications in a tropical location", *Nigeria J. Sust. Res.,* vol. 14, no 5, pp 1-7, 2016.doi: 10.1109/AFRCON.2007.4401597

[27] Guoxu Fenga, Jun Huanga and Zhenbo Wu, "Overcoming geometric issues in the multipath propagation of electromagnetic waves using ray tracing and spherical ground surface theory." *Optik- Int. J. Light Electr, opt.*, vol. 181, pp. 326-337, Mar. 2019, doi: 10.1016/j.ijleo.2018.12.093

[28] B. R. Bean, G.D, Thayer, Models of the atmospheric radio refractive index, *Proc. IRE,* vol. 47, no. 5, pp. 740–755, May 1959, doi: 10.1109/JRPROC.1959.287242

[29] ITU-R, 453-12: The radio refractivity index; its formula and refractivity data, 2016.

[30] J. Gao, K. Brewster, and M. Xue, "Variation of radio refractivity with respect to moisture and temperature and influence on radar ray path," *Adv Atmos Sci.*, vol. 25, no. 6, pp. 1098-1106, Nov. 2008, doi: 10.1007/s00376-008-1098-x

[31] S. M. Yu, L. Yee, Hui and C. N. Boon, "Empirical Near Ground Path Loss Modeling in a Forest at VHF and UHF Bands,". *IEEE Trans. Antennas Propag.*, vol. 57, no. 5, pp 1461 – 1468, May 2009. doi: 10.1109/TAP.2009.2016703

[32] ITU R P. 530 16., Prediction Methods Required for the Design of Terrestrial Line of Sight. 2015.

[33] O. F. Dairo, and L. B. Kolawole, "Radio refractivity gradients in the lowest 100 m of the atmosphere over Lagos, Nigeria in the rainy-harmattan transition phase," *J. Atmos. S. Terr. P.,* vol. 167. No 1 and 2, pp 169-176, Oct. 2017. doi: 10.1016/j.jastp.2017.12.001

[34] ITU-R P.530-17: Propagation data and prediction methods required for the design of terrestrial line-of-sight systems.